

---

# Advances in Electronic Ceramic Materials

---

---

*A collection of papers presented at the  
29th International Conference  
on Advanced Ceramics and Composites,  
January 23-28, 2005,  
Cocoa Beach, Florida*

## Editors

Sheng Yao  
Bruce Tuttle  
Clive Randall  
Dwight Viehland

## General Editors

Dongming Zhu  
Waltraud M. Kriven



Published by

The American Ceramic Society  
735 Ceramic Place  
Suite 100  
Westerville, Ohio 43081  
[www.ceramics.org](http://www.ceramics.org)

The page is intensely left blank

---

# Advances in Electronic Ceramic Materials

---

---

The page is intensely left blank

---

# Advances in Electronic Ceramic Materials

---

---

*A collection of papers presented at the  
29th International Conference  
on Advanced Ceramics and Composites,  
January 23-28, 2005,  
Cocoa Beach, Florida*

## Editors

Sheng Yao  
Bruce Tuttle  
Clive Randall  
Dwight Viehland

## General Editors

Dongming Zhu  
Waltraud M. Kriven



Published by

The American Ceramic Society  
735 Ceramic Place  
Suite 100  
Westerville, Ohio 43081  
[www.ceramics.org](http://www.ceramics.org)

## Advances in Electronic Ceramic Materials

Copyright 2005. The American Ceramic Society. All rights reserved.

Statements of fact and opinion are the responsibility of the authors alone and do not imply an opinion on the part of the officers, staff or members of The American Ceramic Society. The American Ceramic Society assumes no responsibility for the statements and opinions advanced by the contributors to its publications or by the speakers at its programs; nor does The American Ceramic Society assume any liability for losses or injuries suffered by attendees at its meetings. Registered names and trademarks, etc., used in this publication, even without specific indication thereof, are not to be considered unprotected by the law. Mention of trade names of commercial products does not constitute endorsement or recommendation for use by the publishers, editors or authors. Final determination of the suitability of any information, procedure or product for use contemplated by any user, and the manner of that use, is the sole responsibility of the user. This book is intended for informational purposes only. Expert advice should be obtained at all times when implementation is being considered, particularly where hazardous materials or processes are encountered.

No part of this book may be reproduced, stored in a retrieval system or transmitted in any form or by any means, electronic, mechanical, photocopying, microfilming, recording or otherwise, without written permission from the publisher.

Authorization to photocopy for internal or personal use beyond the limits of Sections 107 and 108 of the U.S. Copyright Law is granted by The American Ceramic Society, provided that the appropriate fee is paid directly to the Copyright Clearance Center, Inc., 222 Rosewood Drive, Danvers, MA 01923 U.S.A., [www.copyright.com](http://www.copyright.com). Prior to photocopying items for educational classroom use, please contact Copyright Clearance Center, Inc.

This consent does not extend to copying items for general distribution or for advertising or promotional purposes or to republishing items in whole or in part in any work in any format.

Please direct republication or special copying permission requests to Staff Director, Technical Publications, The American Ceramic Society, 735 Ceramics Place, Suite 100, Westerville, Ohio 43081, USA.

For information on ordering titles published by The American Ceramic Society, or to request a publications catalog, please call 614-794-5890, or visit [www.ceramics.org](http://www.ceramics.org)

ISSN 0196-6219

ISBN 1-57498-235-4

---

# Contents

---

---

Preface .....	ix
<b>Emerging Sensor Technology Based on Electroceramics</b>	
Zirconia-Based Gas Sensors Using Oxide Sensing Electrode for Monitoring NO <sub>x</sub> in Car Exhaust .....	3
N. Miura, J. Wang, M. Nakatou, P. Elumalai, S. Zhuiykov, D. Terada, and T. Ono	
Interfacial Processes of Ion Conducting Ceramic Materials for Advanced Chemical Sensors .....	15
W. Weppner	
Metal-Oxide Based Toxic Gas Sensors .....	25
D.D. Lee and N.J. Choi	
Thermally Stable Mesoporous SnO <sub>2</sub> and TiO <sub>2</sub> Powders for Semi-Conductor Gas Sensor Application .....	37
Y. Shimizu and M. Egashira	
DC Electrical-Biased, All-Oxide NO <sub>x</sub> Sensing Elements for Use at 873 K ...	49
D. West, F. Montgomery, and T. Armstrong	
Photo-Deactivated Room Temperature Hydrogen Gas Sensitivity of Nanocrystalline Doped-Tin Oxide Sensor .....	57
S. Shukla, R. Agrawal, J. Duarte, H. Cho, S. Seal, and L. Ludwig	
PTCR-CO Ceramics as Chemical Sensors .....	65
Z.-G. Zhou, Z.-L. Tang, and Z.-T. Zhang	
Full Range Dynamic Study of Exhaust Gas Oxygen Sensors .....	79
D.Y. Wang and E. Detwiler	

## Advanced Dielectric Materials Phenomena

Dielectric Properties of nm-Sized Barium Titanate Fine Particles and Their Size Dependence .....	89
S. Wada, T. Hoshina, H. Yasuno, M. Ohishi, H. Kakemoto, T. Tsurumi, and M. Yashima	
The Effect of Starting Powders on the Giant Dielectric Properties of the Perovskite $\text{CaCu}_3\text{Ti}_4\text{O}_{12}$ .....	101
B. Bender and M.-J. Pan	
Dielectric and Microstructural Properties of $\text{Ba}(\text{Ti}_{1-x}\text{Zr}_x)\text{O}_3$ Thin Films on Copper Substrates .....	109
J.F. Ihlefeld, J-P. Maria, and W. Borland	
Effect of A-Site Substitutions on the Microstructure and Dielectric Properties of Bismuth Sodium Titanate-Based Ceramics Exhibiting Morphotropic Phase Boundary .....	117
R. Vintila, G. Mendoza-Suarez, J.A. Kozinski, and R.A.L. Drew	
High Q ( $\text{Ba}$ , $\text{Sr}$ ) $\text{TiO}_3$ Interdigitated Capacitors Fabricated on Low Cost Polycrystalline Alumina Substrates with Copper Metallization .....	125
D. Ghosh, B. Laughlin, J. Nath, A.I. Kingon, M.B. Steer, and J.-P. Maria	
<b>Microwave Dielectric Materials</b>	
Ionic Distribution and Microwave Dielectric Properties for Tungstenbronze-Type Like $\text{Ba}_{6-3x}\text{R}_{8+2x}\text{Ti}_{18}\text{O}_{54}$ ( $\text{R} = \text{Sm}$ , $\text{Nd}$ and $\text{La}$ ) Solid Solutions .....	135
H. Ohsato, M. Suzuki, and K. Kakimoto	
Crystal Structure Analysis of Homologous Compounds $\text{ALa}_4\text{Ti}_4\text{O}_{15}$ ( $\text{A}=\text{Ba}$ , $\text{Sr}$ and $\text{Ca}$ ) and Their Microwave Dielectric Properties .....	147
Y. Tohdo, K. Kakimoto, H. Ohsato, T. Okawa, and H. Okabe	
Effects of Ionic Radii and Polarizability on the Microwave Dielectric Properties of Forsterite Solid Solutions .....	155
T. Sugiyama, H. Ohsato, T. Tsunooka, and K. Kakimoto	
Microwave Characterization of Calcium Fluoride in the Temperature Range 15-300K .....	161
M.V. Jacob, J. Mazierska, and J. Krupka	
High-Quality 2 Inch $\text{La}_3\text{Ga}_{5.5}\text{Ta}_{0.5}\text{O}_{14}$ and $\text{Ca}_3\text{TaGa}_3\text{Si}_2\text{O}_{14}$ Crystals for Oscillators and Resonators .....	169
C.F. Klemenz, J. Luo, and D. Shah	



Growth of LaAlO <sub>3</sub> Single Crystal by Floating Zone Method and its Microwave Properties . . . . .	177
S. Suzuki, H. Ohsato, K.-I. Kakimoto, T. Shimada, K. Sasaki, and H. Saka	
<b>General Topics in Electronic Ceramics</b>	
Effects of Niobium Addition on Microstructural and Electrical Properties of Lead Zirconate Titanate Solid Solution (PZT 95/5) . . . . .	187
P. Yang, J.A. Voigt, M.A. Rodriguez, R.H. Moore, and G.R. Burns	
Enhanced Density and Piezoelectric Anisotropy in High T <sub>c</sub> PbNb <sub>2</sub> O <sub>6</sub> Based Ferroelectric Ceramics . . . . .	197
D. Garcia, M. Venet, A. Vendramini, J.A. Eiras, and F. Guerrero	
Electrical Properties of Quaternary Pyrochlore Ruthenates for Thick-Film Resistors . . . . .	203
K. Yokoyama, K. Kakimoto, H. Ohsato, J. Kinoshita, and Y. Maeda	
Measurement of Complex Permittivity of Low Temperature Co-Fired Ceramic at Cryogenic Temperatures . . . . .	209
M.V. Jacob, J. Mazierska, and M. Bialkowski	
Author Index . . . . .	217

The page is intensely left blank

---

# Preface

---

*The Electronics Division of the American Ceramic Society sponsored two different electronic ceramics symposia at the 29th International Conference on Advanced Ceramics and Composites organized by the Engineering Division of the American Ceramic Society. This proceedings contains selected papers from the two symposia: (1) Emerging Sensor Technologies Based on Electroceramics and (2) Advanced Dielectric, Piezoelectric and Ferroelectric Materials.*

*The symposium on Emerging Sensor Technologies Based on Electroceramics proved to be a magnificent opportunity to discuss the latest breakthroughs in the field of sensor science and technology. With over 80% of the top scientists in the world in the ceramic sensor field gathered in one room on beautiful Cocoa Beach, it was truly a monumental event. Nowadays, sensor technology is widely used in many applications including critical care, industrial process control, emission monitoring, automotive and home security systems, and more recently, for homeland security. It has undoubtedly made a considerable impact on modern society and human life. The economic and social benefits of sensor technology are evident and multifaceted. In particular, because of the excellent thermal stability of ceramic materials, ceramic sensors have been shown to provide a promising gas detection methodology in harsh environments such as engine and fuel cell exhausts. These currently receive much attention for environmental protection and hence became one of the important topics in this symposium.*

*Sensor technology is largely dependent on the progress made in the field of material science. In this sensor symposium, for example, several reports discussed new catalysts to modify sensing electrodes of non-Nernstian type sensors and semiconducting ceramic sensors; big improvements in sensing performance have been achieved. Several new solid electrolyte materials have been developed and showed to be promising for constructing sensors. New nano-structured materials and SiC based high temperature ceramics showed unique properties for chemical sensing. Therefore, great progress in sensor technology has been made through developing and employing novel materials. In fact, sensors are becoming increasingly important in ceramic material applications. Constructive discussions and communications such as this symposium will advance unequivocally our understanding and perspective on sensor science.*

*The Advanced Dielectric, Piezoelectric and Ferroelectric Materials Symposium brought together researchers and engineers from Europe, Asia, North America and Australia to present and exchange ideas on the latest scientific and technical developments in the field of dielectric, ferroelectric and piezoelectric ceramics. Seventy-four papers and posters were presented. A particular strength of this meeting was the ample opportunity for informal, lively discussions of technical subjects among the meeting participants. Among the topics that attracted a great deal of interest were*

*the latest materials science discoveries for high dielectric constant copper calcium titanate materials, novel high temperature piezoelectrics, fundamental understanding of crystal structure and sub-nanometer distortions on microwave properties, and integration of Cu electrodes with BaTiO<sub>3</sub> and PZT based thin films.*

*We gratefully acknowledged the efforts of the organizing committee for putting together a technical program that drew leading technical experts throughout the world as symposium speakers. We are also extremely grateful to all the speakers who contributed to this highly successful symposium, especially those from outside of North America.*

*Sheng Yao  
Emerging Sensor Technologies Based on Electroceramics*

*Bruce Tuttle, Clive Randall and Dwight Viehland  
Advanced Dielectric, Piezoelectric and Ferroelectric Materials*

---

# Emerging Sensor Technology Based on Electroceramics

---

---

The page is intensely left blank

# ZIRCONIA-BASED GAS SENSORS USING OXIDE SENSING ELECTRODE FOR MONITORING NO<sub>x</sub> IN CAR EXHAUST

N. Miura, J. Wang, M. Nakatou, P. Elumalai, S. Zhuiykov and D. Terada  
Art, Science and Technology Center for Cooperative Research, Kyushu University,  
Kasuga-shi, Fukuoka 816-8580, JAPAN  
T. Ono  
R&D Division, Riken Corporation, Kumagaya-shi, Saitama 360-8522, JAPAN

## ABSTRACT

Solid-state electrochemical sensors using yttria-stabilized zirconia (YSZ) and oxide sensing electrode (SE) were fabricated and examined for NO<sub>x</sub> detection at high temperatures. Among various single-oxide SEs examined, NiO-SE for the mixed-potential-type NO<sub>x</sub> sensor was found to exhibit rather high sensitivity to NO<sub>2</sub> even in the high temperature range of 800-900°C. This sensor showed quicker response and recovery transients in the presence of water vapor, compared with that in the dry sample gas. The sensing mechanism of this type of sensor was discussed on the basis of the catalytic activities to the electrochemical and non-electrochemical reactions. It was also shown that the new-type complex-impedance-based (impedancemetric) NO<sub>x</sub> sensor attached with ZnCr<sub>2</sub>O<sub>4</sub>-SE exhibit good sensing characteristics to NO<sub>x</sub> at 700°C. Furthermore, the sensitivity to NO was almost equal to that to NO<sub>2</sub> in the concentration range from 0 to ca. 200 ppm at 700°C. A linear dependence was observed between the sensitivity of the impedancemetric sensor and the concentration of NO<sub>x</sub> even in the presence of 8 vol. % H<sub>2</sub>O and 15 vol.% CO<sub>2</sub>. The planar laminated-type structure for the impedancemetric NO<sub>x</sub> sensor was proposed for protecting NO<sub>x</sub> sensitivity from the influences of the co-existing combustible gases as well as the change in oxygen concentration in exhaust gas.

## INTRODUCTION

Recently, the demand for reliable, compact, low-cost solid-state sensors, which are capable of detecting nitrogen oxides (NO<sub>x</sub>) in different application, has been enhanced substantially. This demand has been driven by strong recent legislation in EU, USA and Japan. For example, in UK under Air Quality Regulations (1997) for NO<sub>x</sub>, standards of 150 *ppb* (hourly maximum) and 21 *ppb* (annual average) must be achieved by the end of 2005.<sup>1</sup> On the other hand, according to a new report by Fredonia Group, US demand for sensor products (including sensors, transducers and associated housing) is projected to increase 7.8% annually to \$13.8 billion in 2008.<sup>2</sup> For monitoring in the automotive exhausts, the sensor should be able to detect NO<sub>x</sub> concentration from 10 ppm up to 2000 ppm in very harsh environment where the temperature constantly fluctuates from 600°C up to 900°C, since the temperature of engine may occasionally reach up to 900°C, during vehicle acceleration. It is therefore vital to investigate thoroughly the SE materials of the NO<sub>x</sub> sensor in order to provide high NO<sub>x</sub> sensitivity and selectivity, long-term stability at high temperatures as well as fast response and recovery for a practical sensor.

---

To the extent authorized under the laws of the United States of America, all copyright interests in this publication are the property of The American Ceramic Society. Any duplication, reproduction, or republication of this publication or any part thereof, without the express written consent of The American Ceramic Society or fee paid to the Copyright Clearance Center, is prohibited.

Last decade, an ultra lean-burn (or direct-injection type) engine system has been developed to improve fuel efficiency as well as to reduce CO<sub>2</sub> and NO<sub>x</sub> emissions from engine. In this engine system, newly-developed NO<sub>x</sub>-storage catalyst should be used for compensating the low NO<sub>x</sub>-removal ability of the conventional three-way catalyst under the lean-burn (air rich) condition, as shown in Fig. 1.<sup>3</sup> It is important, therefore, to have high-performance NO<sub>x</sub> sensors installed at the point after (or both before and after) the NO<sub>x</sub>-storage catalyst for such a system.

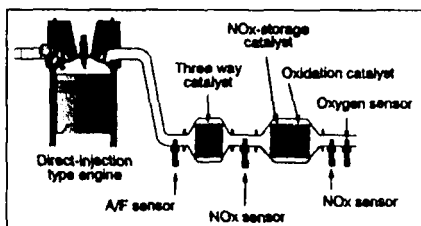


Fig. 1 Catalytic converter system equipped with NO<sub>x</sub> sensors for the exhaust gas emitted from a new-type car engine.

The mixed-potential-type NO<sub>x</sub> sensors based on YSZ and oxide SE have been receiving considerable attention among the others YSZ-based NO<sub>x</sub> sensors,<sup>4</sup> as potential candidates for practical sensor measuring car emissions. For example, last few years the most of the research groups have focused on the development of oxide SEs which are capable of working at high temperatures in car exhaust.<sup>5-9</sup> The use of oxide SE in this type of NO<sub>x</sub> sensor was found to be very effective for sensitive and selective NO<sub>x</sub> measurement at high temperature.<sup>10</sup> However, there are only a few designs of the NO<sub>x</sub> sensors reported to date<sup>11-16</sup> that can monitor total NO<sub>x</sub> (NO + NO<sub>2</sub>) at high temperatures regardless of NO<sub>2</sub>/NO ratio in real exhausts. One of these sensors is the complex-impedance-based NO<sub>x</sub> sensor originally designed and developed by our group.<sup>15,16</sup> In addition, the most of results for oxide SEs published so far have revealed that the NO<sub>x</sub> sensors using the oxide SEs show relatively good sensing characteristics only in the temperature range of 450-700°C. The majority of these sensors have difficulty to operate at temperatures higher than 700°C. Such a higher limitation of operating temperature is caused by the substantial decrease in the NO<sub>x</sub> sensitivity with increasing temperature. Based on the above-mentioned facts and keeping it in mind that there are no commercial high-temperature NO<sub>x</sub> sensors available on the market at the moment, further search for oxide SE has been done. As a result, it was found quite recently that NiO is a very effective SE for measuring NO<sub>x</sub> concentrations at temperatures higher than 800°C.<sup>17,18</sup> There were only limited number of publications reporting the properties and sensing characteristics of oxide SE that can measure NO<sub>x</sub> concentration at temperatures over 800°C.<sup>17,18</sup> Furthermore, we have also discovered that the new complex-impedance-type NO<sub>x</sub> sensor using ZnCr<sub>2</sub>O<sub>4</sub>-SE shows rather good sensing characteristics for measurement of total NO<sub>x</sub> concentration at temperature as high as 700°C. Thus, we report here the sensing properties and sensing mechanism of the mixed-potential-type YSZ-based NO<sub>x</sub> sensor attached with NiO-SE at temperatures of 800-900°C as well as the main sensing performances of the new complex-impedance-type NO<sub>x</sub> sensor using ZnCr<sub>2</sub>O<sub>4</sub>-SE.

## EXPERIMENTAL

A tubular NO<sub>x</sub> sensor was fabricated by using a commercial one-closed-end YSZ tube (8 wt.% Y<sub>2</sub>O<sub>3</sub>-doped, NKT). The tube is 300 mm in length and 5 and 8 mm in inner and outer diameters, respectively. NiO-powder paste was applied on the outer surface of the YSZ tube and sintered at 1400°C to form a sensing electrode (SE). A Pt lead wire was wound around the oxide layer to make a good electrical contact. Pt paste was painted onto the inside of the YSZ



tube and fired afterwards at 1000°C for 2 h to form a reference electrode (RE). Figure 2 shows the cross-sectional (schematic) view of the obtained tubular YSZ sensor attached with NiO-SE and Pt-RE.

The fabrication of planar NO<sub>x</sub> sensor was done by the use of YSZ plates (8 wt. % Y<sub>2</sub>O<sub>3</sub>-doped, 10 x 10 mm; 0.2 mm thickness). Pt paste was printed on both sides of the YSZ plate and then was fired at 1000°C for 2 h in air. On the one side of the YSZ plate, two rectangular Pt-strips were formed as Pt-RE of the sensor and, on the other side; six narrow Pt-strips were formed as a base (current collector) for the NiO-SE film. NiO powder (Kojundo Chemical Lab. Co. Ltd., 99.97% purity) was thoroughly mixed with  $\alpha$ -terpineol (20 wt.%) and the resulting paste was applied on the top side of the YSZ plate attached with narrow Pt-strips by means of screen-printing technique to form SE. The planar sensors were sintered at 1100°C, 1200°C, 1300°C and 1400°C, respectively, for 2 h in air. Although the Pt-RE of the tubular YSZ-based NO<sub>x</sub> sensors has been always exposed to the atmospheric air during experiments,<sup>19</sup> the Pt-RE of the present planar sensor is always exposed to the measuring gas. Pt wires were spot-welded onto the Pt connecting-spots of both SE and one of REs to provide the good electrical contact with a measuring equipment.

The microstructure and surface topography of the NiO-SE films were examined by using an SEM (JEOL electron microscope, JSM-340F) operating at 15 kV. The crystal structure of the films was studied by means of a wide-angle XRD (RIGAKU X-ray diffractometer, RINT 2100VLR/PC). The CuK $\alpha$  radiation ( $\lambda=1.5406$ ) and 0.5°/min angle step were used for the XRD measurement. The YSZ/NiO interface was observed by the use of a TEM (FEI Inc., Model TECNAI F20) at the Research Laboratory for High Voltage Electron Microscopy of Kyushu University. The accelerated voltage was 200 kV for all experiments. BET surface area was measured by using an automated gas-sorption system (Quantachrome Autosorb, version 1.20).

NO<sub>x</sub>-sensing experiments were carried out in a conventional gas-flow apparatus operating in the temperature range of 700-900°C, as shown in Fig. 3. The sample gas containing various concentrations of NO (or NO<sub>2</sub>) was prepared by diluting with dry nitrogen and oxygen gases and was allowed to flow over the sensor at a constant flow rate of 100 cm<sup>3</sup> min<sup>-1</sup>. The concentrations of NO and NO<sub>2</sub> were changed from 10 to 400 ppm. The difference in potential (emf) between NiO-SE and Pt-RE of the sensor was measured by a digital electrometer (Advantest, R8240). The base gas was 5 or 20.9 vol.% of dry O<sub>2</sub> diluted with dry N<sub>2</sub>, and the sample gas was 10-400 ppm of NO<sub>x</sub> diluted with the base gas. In

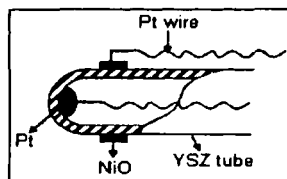


Fig. 2 Cross-sectional (schematic) view of the tubular YSZ sensor.

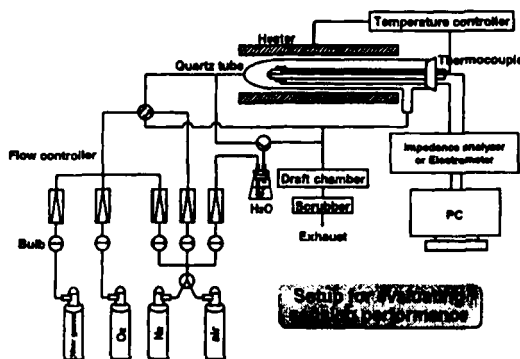


Fig. 3 Setup for evaluating sensing performances of NO<sub>x</sub> sensors.

order to humidify the base gas and the sample gas, 5 vol.% water vapor was mixed with them. For the impedance-based sensor, the complex impedance and the phase angle between SE and RE were measured with a complex impedance analyzer (Solartron, 1255 WB) in the frequency range of 0.01 Hz - 1 MHz to obtain complex-impedance (Nyquist) plots. As an output signal, the complex impedance value ( $|Z|$ ) was used and was monitored at a fixed frequency of 1 Hz.

## RESULTS AND DISCUSSION

### Crystal Structure and Morphology of the Oxide SEs

One of the most important factors that affect the sensing characteristics of the mixed-potential-type NO<sub>x</sub> sensors is the composition or morphology of SE. XRD patterns for both NiO and ZnCr<sub>2</sub>O<sub>4</sub> thick films sintered at 1400°C and 1200°C, respectively, contained only peaks of crystalline face-centered cubic NiO (JCPDS PDF#47-1049) phase or ZnCr<sub>2</sub>O<sub>4</sub> (JCPDS PDF#22-1107) phase. It is seen that all peaks for the sintered NiO and ZnCr<sub>2</sub>O<sub>4</sub> were narrow. This suggests the excellent thermal stability of NiO and ZnCr<sub>2</sub>O<sub>4</sub>.

Figure 4 shows SEM micrographs of the cross-section of the screen-printed NiO-SE films sintered at different temperatures on the YSZ substrate. The thickness of films was maintained at almost same value of about 7 μm even after sintering at different temperatures. With decreasing sintering temperature, the average pore size was found to increase from *ca.* 0.5 μm (for the 1100°C-sintered film) to *ca.* 2 μm (for the 1400°C-sintered film). This suggests that higher sintering temperature gives lower number of reaction site at a triple-phase-boundary (TPB) of gas/YSZ/NiO. These observations also show that the high sintering temperature provides relatively low surface-to-volume ratio on SE layer which consequently brings low catalytic activity to electrochemical reactions. The less surface area of the NiO film will also lead to lower heterogeneous catalysis (decomposition of NO<sub>2</sub> to NO). In the case of the ZnCr<sub>2</sub>O<sub>4</sub>-SE sintered at 1200°C, it was also relatively porous with an average grains size of about 0.2-0.8 μm.

TEM image of the TPB (gas/YSZ/SE) for the NiO-SE sintered at 1400°C onto YSZ substrate is presented in Fig. 5. Analysis of this figure showed that the TPB, where all electrochemical reactions occur, is a small

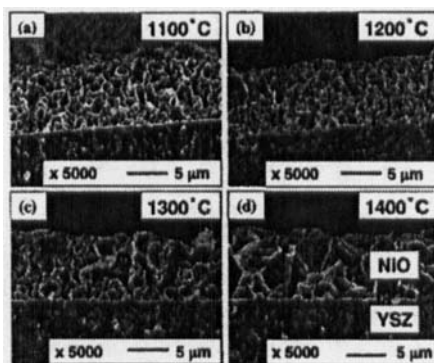


Fig. 4 SEM micrographs of the cross-section of the screen-printed NiO films (on YSZ substrate) sintered at various temperatures.

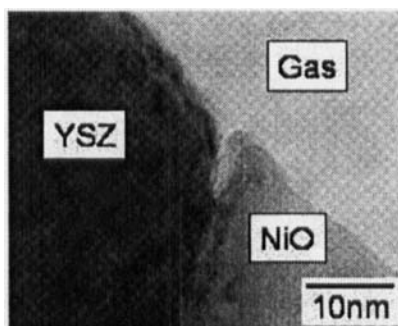


Fig. 5 TEM micrograph of the TPB at gas/YSZ/NiO for the NiO film sintered onto YSZ substrate at 1400°C.

curve which goes along with the YSZ/NiO interface. This nano-scale picture clearly shows that the YSZ/NiO interface is about 2 nm in thickness and goes along the boundary between the NiO and YSZ grains joined together. Thus, the TPB consists of the gas and the combination of the relatively small nano-scale curves along the YSZ/NiO interface as well as small islands when the YSZ and NiO grains connected to each other by one or a few single points.

#### Sensing Performances of the Mixed-potential-type NO<sub>x</sub> Sensor Using NiO-SE

Among the thirteen kinds of single-oxide SEs tested, the NiO-SE was found to give the highest NO<sub>2</sub> sensitivity at 850°C. The YSZ-based NO<sub>x</sub> sensor attached with NiO-SE showed a strong linear correlation between the gas sensitivity and the logarithm of NO<sub>2</sub> concentration from 50 ppm up to 450 ppm at temperatures of 800-900°C. Figure 6 shows the variation of the output emf values for the present sensor to 400 ppm NO<sub>x</sub> (NO or NO<sub>2</sub>) when the operating temperature was changed from 800°C up to 900°C. The oxygen concentration was fixed at 20.9 vol.%. It is clear from this figure that the output emf of the NO<sub>x</sub>

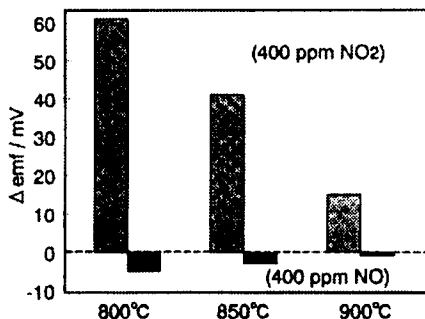


Fig. 6 Variation of the output emf for the NO<sub>x</sub> sensor using NiO-SE at operating temperatures of 800-900°C.

sensor decreases with increasing operating temperature. However, even at 900°C the sensor attached with NiO-SE gave the emf response of about 15 mV. Such a result is hard to see in the case of any other oxide-SEs tested here and reported to date. Figure 7 shows the response transients to 400 ppm NO<sub>2</sub> under dry and wet conditions for the tubular NO<sub>x</sub> sensor attached with NiO-SE at 850°C. The emf value was almost zero when the base gas was introduced to the sensor and changed quickly from the base level to the some emf value upon exposure to the sample gas containing NO<sub>2</sub>. The 90% response time was about 40 s, however the recovery rate was very slow compared with the response rate. The emf value did not return to the base level and reached only the about 80% recovery level even after 20 min. Such a slow recovery can be explained by the fact that the catalytic activity for electrochemical reaction of oxygen ( $\frac{1}{2}\text{O}_2 + 2e^- = \text{O}^{2-}$ ) is low for the 1400°C-sintered NiO-SE. Such a slow recovery of the present sensor was found to be improved by humidifying the sample gas. In this test, 5 vol.% of water vapor was incorporated into the dry sample gas. As shown in Fig. 7 (b), the recovery rate was greatly improved after the introduction of water vapor. Under the wet condition, the 90% response and 90% recovery times were about 20 s and about 3 min, respectively. The emf value returned completely to the original level within about 5 min. In addition, the sensitivity (75 mV to 400 ppm NO<sub>2</sub>) under

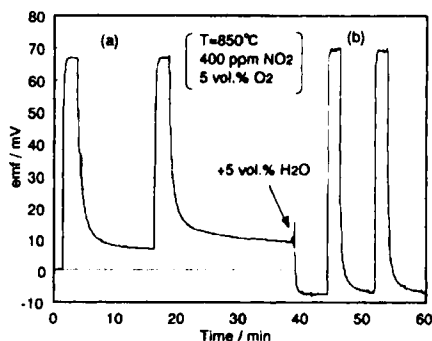


Fig. 7 Response/recovery transients to 400 ppm NO<sub>2</sub> in 5 vol.% O<sub>2</sub> (+N<sub>2</sub> balance) gas in the absence (a) and in the presence (b) of 5 vol.% water vapor at 850°C.

the wet condition was a bit higher than that (60 mV) under the dry condition. Moreover, the reproducibility of emf response to 400 ppm NO<sub>2</sub> was quite satisfactory. Thus, the presence of water vapor in car exhausts will give a positive effect to the performance of the present NO<sub>x</sub> sensor.

Figure 8 shows the comparison of the response transients to 200 ppm NO<sub>2</sub> at 800°C for the planar sensors attached with each of NiO-SEs sintered at various temperatures. It is seen that the steady-state emf value to 200 ppm NO<sub>2</sub> increased from 3 mV to 55 mV when the sintering temperature of SE was increased from 1100 to 1400°C. However, the response rate was lowered by increasing the sintering temperature. These results given in Fig. 8 clearly indicate that the NO<sub>2</sub> sensitivity of the present sensor can be enhanced by increasing the sintering temperature of SE.

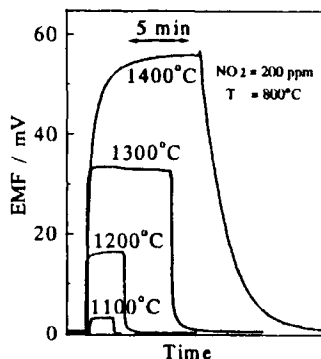
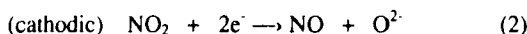
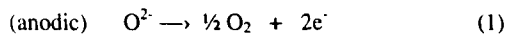


Fig. 8 Response transients to NO<sub>2</sub> at 800°C for the planar sensors using each of NiO-SEs sintered at different temperatures.

#### Elucidation of Sensing Mechanism for the Mixed-potential-type NO<sub>2</sub> Sensor

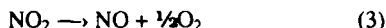
The NO<sub>x</sub> sensing mechanism for the YSZ-based sensors using metal-oxide SE is based on mixed-potential, as has been reported before.<sup>8,17</sup> For the NO<sub>2</sub> sensing, the following electrochemical reactions proceed simultaneously at the interface of YSZ/SE and consequently mixed potential appears on SE:



Based on the previously published results,<sup>3,4,10</sup> these reactions occur at different kinetic rates on the dissimilar electrodes. As a result, the emf response of the sensor is the difference in mixed potential on each electrode. Therefore, the catalytic activity to anodic reaction of O<sub>2</sub> (1) should be low and the catalytic activity to cathodic reaction of NO<sub>2</sub> (2) should be high. In order to verify this assumption, the complex impedance measurements were performed at the frequency range of 0.01 Hz <math>\ll</math> MHz in the base gas (5 vol.% O<sub>2</sub> + N<sub>2</sub> balance) at 800°C for the planar sensors attached with each of the NiO-SEs sintered at different temperatures. It was seen that the resistance of electrode reaction in the base gas increased with increasing sintering temperature of SE. This implies that the higher sintering temperature of SE gives lower catalytic activity to anodic reaction of oxygen (1). The decrease in the catalytic activity to the anodic reaction in the case of higher sintering temperature of SE was also confirmed from the results of the polarization-curve measurements. At the same time, the low catalytic activity to the cathodic reaction of NO<sub>2</sub> (2) can be explained using the schematic view of the interface shown in Fig. 9. One can see that smaller NiO grains are present at TPB in the case of lower sintering temperature of SE. In contrast, larger grains are present at TPB in the case of higher sintering temperature. The larger grains may produce less number of reaction sites at TPB. Thus, we can speculate that, in the case of higher sintering temperature, the catalytic activity to

the cathodic reaction (2) is low compared to the case of lower sintering temperature, as observed for the anodic reaction.

Moreover, the oxide matrix also plays an important role in deciding the  $\text{NO}_2$  sensitivity<sup>17</sup> when we consider the gas-phase reaction:



Based on our previous results,<sup>3,5,19</sup> low conversion of  $\text{NO}_2$  in the gas-phase reaction would lead to high  $\text{NO}_2$  sensitivity. In the present study, it was observed from the SEM images (see Fig. 4) that the large pores exist in the case of the 1400°C-sintered NiO-SE. As shown in Fig. 9,  $\text{NO}_2$  gas makes less contacts with the surface of NiO grains when it diffuses through the large pores presenting in the 1400°C-sintered SE matrix, where its surface acts as a catalyst for gas-phase decomposition reaction of  $\text{NO}_2$  (3). Thus,  $\text{NO}_2$  can reach the YSZ/SE interface without serious decomposition to NO. In contrast,  $\text{NO}_2$  makes a significant contacts with the surface of NiO grains when it diffuses through the small pores presenting in the 1100°C-sintered SE matrix where almost all  $\text{NO}_2$  gas can be converted into NO before reaching the TPB. Thus, the low catalytic activity to anodic reaction of oxygen as well as less possible conversion of  $\text{NO}_2$  to NO in the gas-phase reaction would lead to higher  $\text{NO}_2$  sensitivity in the case of the 1400°C-sintered SE. Furthermore, the high catalytic activity for the anodic reaction of oxygen and the high conversion of  $\text{NO}_2$  to NO lead to lower  $\text{NO}_2$  sensitivity in the case of the 1100°C-sintered SE, in spite of the fact that the high catalytic activity to anodic reaction of oxygen can give faster recovery rate.

All the above results presented here show that NiO-SE gives good sensing performances in the humid exhaust environment even at high temperatures of 800-900°C. Thus, we may conclude that this material is one of the potential candidates for SE of the mixed-potential-type  $\text{NO}_x$  sensor which is capable of detecting  $\text{NO}_x$  on-board in car exhausts at high temperature.

### Sensing Performances of the Complex Impedance-based $\text{NO}_x$ Sensor

In addition to the mixed-potential-type  $\text{NO}_x$  sensors, our attention during last few years has been focusing on the development of principally new-type YSZ-based sensor for detecting  $\text{NO}_x$  at high temperature.<sup>3,16</sup> In this type of  $\text{NO}_x$  sensors, the change in the complex impedance of the device attached with oxide SE was measured as a sensing signal. Initially we investigated the complex-impedance plots for the devices using spinel-type oxides, such as  $\text{CrMn}_2\text{O}_4$ ,  $\text{NiCr}_2\text{O}_4$ ,  $\text{NiFe}_2\text{O}_4$  and  $\text{ZnCr}_2\text{O}_4$ , as an SE in base air at 700°C. Both  $\text{NO}_2$  and NO (200 ppm each, diluted with dry air) were used as the sample gas during experiments. The sensors attached with the first three oxides were found to provide large and flat semicircular arc in each Nyquist plots in the examined frequency range. The impedance values of these devices were not affected by the existence of  $\text{NO}_x$  under the present condition. However, we found that in the case of the device attached with  $\text{ZnCr}_2\text{O}_4$ -SE, the impedance behavior was

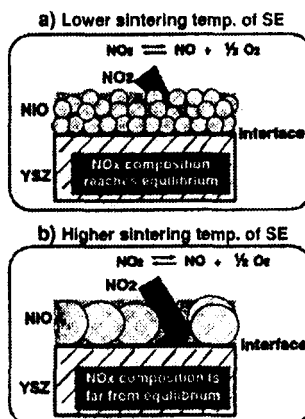


Fig. 9 Schematic views of the effect of both grain size and pore size of the SE matrix on catalytic activities to reactions (1) and (3).

entirely different from the above-mentioned results. Figure 10 shows how the resistance value ( $Z'$ , the intercept) at the intersection of the large semi-arc with the real axis at low frequencies (around 0.1 Hz) varies with concentrations of both NO and NO<sub>2</sub>. It is seen that the resistance value decreases with an increase in the concentration of both NO and NO<sub>2</sub>. Such a behavior is completely different from that for the mixed-potential-type NO<sub>x</sub> sensor whose response direction to NO is opposite to that to NO<sub>2</sub> (see Fig. 6).

Meanwhile, the  $Z'$  value (the intercept, about 2000 Ohm) at the intersection of the large semi-arc at high frequencies (around 50 kHz) did not change even if the concentration of NO<sub>x</sub> was changed from 10 to 400 ppm. The difference between the impedance ( $|Z|_{\text{air}}$ ) in the base air and the impedance ( $|Z|_{\text{gas}}$ )

in the sample gas containing NO<sub>x</sub> at the fixed frequency of 1 Hz has been defined as 'gas sensitivity' of the device.<sup>3, 15, 16</sup> We, therefore, investigated the sensitivity of sensor attached with ZnCr<sub>2</sub>O<sub>4</sub>-SE to both NO and NO<sub>2</sub> at high temperature and in the presence of high concentration of H<sub>2</sub>O (3 to 8 vol.%) and CO<sub>2</sub> (10 to 15 vol.%), which are usually exist in car exhausts. All measurements were carried out at fixed temperature of 700°C for various NO<sub>x</sub> concentrations. This investigation revealed the existence of strong linear correlation between 'gas sensitivity' and the measuring NO<sub>x</sub> concentration from 0 to 200 ppm. Figure 11 shows that the sensitivity of the sensor at 1 Hz to both NO and NO<sub>2</sub> (200 ppm each) was almost constant in the presence of high H<sub>2</sub>O and CO<sub>2</sub> concentrations. Moreover, the most interesting result taken into consideration from these tests is the fact that the sensitivity to NO is almost equal to that to NO<sub>2</sub> at 700°C. From the practical point of view, this means that the present device is capable of measuring total NO<sub>x</sub> (NO and NO<sub>2</sub>) concentration in the gas mixture regardless of the NO/NO<sub>2</sub> ratio. This is very valuable point for the development of practical total NO<sub>x</sub> sensor for car exhausts.

Based on our previous experiences with the mixed-potential-type sensors, we can presume that it

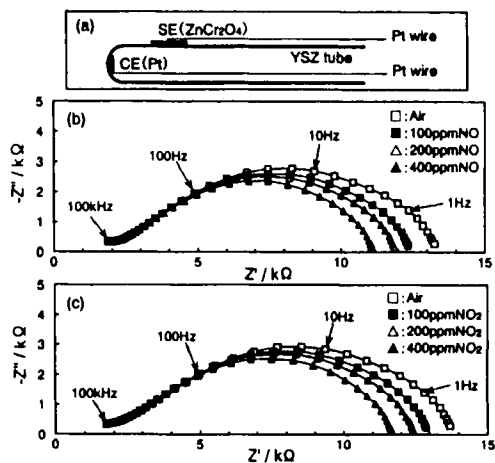


Fig. 10 (a) Cross-sectional view of the complex impedance-based NO<sub>x</sub> sensor using YSZ and ZnCr<sub>2</sub>O<sub>4</sub>-SE. (b), (c) Nyquist plots in the base air and the sample gas with each of various concentrations of NO and NO<sub>2</sub> at 700°C.

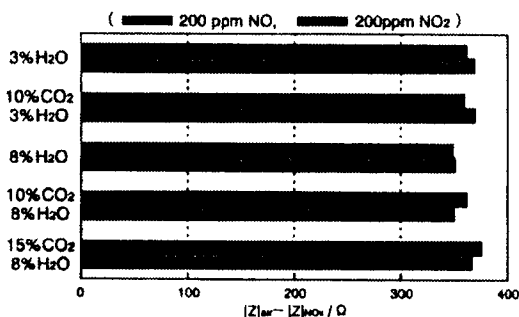


Fig. 11 Sensitivity to NO and NO<sub>2</sub> (200 ppm each) in the presence of rather high concentrations of H<sub>2</sub>O (3-8 vol.%) and CO<sub>2</sub> (10-15 vol.%) at 700°C for the YSZ-based sensor using ZnCr<sub>2</sub>O<sub>4</sub>-SE.

is quite possible that the response of the present device is also intervened by the change in  $O_2$  concentration in the sample gas.

In order to verify this assumption,  $O_2$  concentration in the sample gas was changed from 5 vol.% to 80 vol.% at  $700^\circ\text{C}$  whilst 'gas sensitivity' of the device to 100 ppm of both NO and  $\text{NO}_2$  was recorded. The results of these tests revealed that the value  $|Z|$  indeed varied linearly with the logarithm of  $O_2$  concentration at 1 Hz. In the meantime, the 'gas sensitivities' to NO and to  $\text{NO}_2$  were almost equal at any  $O_2$  concentration examined. This suggests that the  $O_2$  concentration in the sample gas existing at the space near the oxide-SE of the device should be controlled and should be kept constant during operation. For this purpose, both an  $O_2$  sensor and an  $O_2$ -pump could be employed for monitoring and controlling  $O_2$  concentration, respectively. These devices can be built into a new laminated-type YSZ-based device consisting of oxidation catalyst and  $\text{NO}_2$  sensing electrode, as shown in Fig. 12. Combustible gases, therefore, can be oxidized by oxidation catalyst in this design of the sensor and the  $O_2$  concentration can be kept constant. Consequently, the  $\text{NO}_x$  sensitivity of the sensor will have no influence by the co-existence of combustible gases and by the  $O_2$  concentration variation in the exhaust gas.

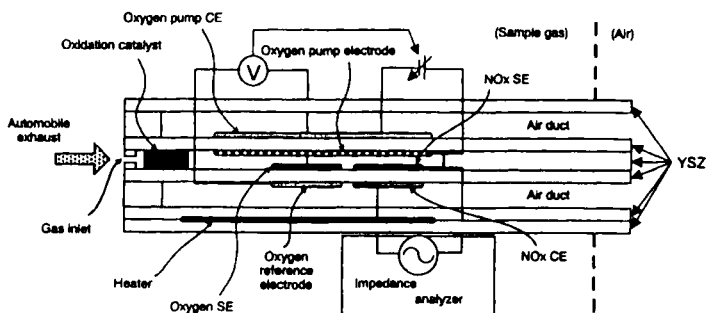


Fig. 12 A cross-sectional view of the proposed laminated-type complex impedance-based  $\text{NO}_x$  sensor.

## CONCLUSIONS

First, the tubular and planar YSZ-based sensors attached with each of the NiO-SEs sintered at various temperatures were fabricated for  $\text{NO}_x$  detection at the different environments aiming for monitoring car exhausts. The sensing characteristics of these sensors were examined in the temperature range of  $800\text{--}900^\circ\text{C}$ . It was found that the  $\text{NO}_2$  sensitivity of NiO-SEs was greatly influenced by changing the sintering temperature of SE. Rather high sensitivity to  $\text{NO}_2$  was obtained even at  $900^\circ\text{C}$  for the sensor using the NiO-SE sintered at  $1400^\circ\text{C}$ . The  $\text{NO}_2$  sensitivity observed at such a high temperature has never been reported before. The low catalytic activity to anodic reaction of oxygen (1) as well as the scanty conversion of  $\text{NO}_2$  to NO on the gas-phase reaction (3) may lead to the high  $\text{NO}_2$  sensitivity in the case of  $1400^\circ\text{C}$ -sintered SE having larger pores. In opposite, the high catalytic activity to anodic reaction and the high conversion of  $\text{NO}_2$  to NO may lead to lower sensitivity in the case of  $1100^\circ\text{C}$ -sintered SE having smaller pores and smaller grains. The present investigation indicates that NiO is a promising candidate for the practical SE of on-board planar  $\text{NO}_x$